Hindawi
Advances in Materials Science and Engineering
Volume 2021, Article ID 5522025, 13 pages
https://doi.org/10.1155/2021/5522025

Research Article

Laboratory Evaluation of Rheological Properties of Asphalt Binder Modified by Nano-TiO_2/$CaCO_3$

Liming Zhang,[1,2] **Xuekai Gao**,[3] **Wensheng Wang**,[1] **Hua Wang**,[4,5] **and Kunkun Zheng**[6]

[1]*College of Transportation, Jilin University, Changchun 130025, China*
[2]*Guangxi Xinfazhan Communication Group Co. Ltd., Nanning 530007, China*
[3]*Key Laboratory of Highway Construction and Maintenance Technology of Ministry of Transport in Loess Region, Shanxi Transportation Technology Research & Development Co. Ltd., Taiyuan 030006, China*
[4]*Guangxi Beibu Gulf Investment Group Co. Ltd., Nanning 530029, China*
[5]*Guangxi Transportation Science and Technology Group Co. Ltd., Nanning 530007, China*
[6]*Guangdong Aohong Technology Co. Ltd., Zhongshan 528437, China*

Correspondence should be addressed to Wensheng Wang; wangws@jlu.edu.cn and Hua Wang; wanghua15@mails.jlu.edu.cn

Received 11 January 2021; Revised 21 January 2021; Accepted 2 February 2021; Published 12 February 2021

Academic Editor: Shuaicheng Guo

Nanomaterials have a great potential for enhancing the performance of base asphalt binder. This study aims to promote the application of nano-TiO_2/$CaCO_3$ in bitumen and presents a study on rheological properties for TiO_2/$CaCO_3$ nanoparticle-bitumen. In this study, a series of laboratory experiments have been performed for bitumen with different nano-TiO_2/$CaCO_3$ dosages. Nano-TiO_2/$CaCO_3$-modified bitumen with optimum dosage was prepared for viscosity, dynamic shear rheometer (DSR), and beam bending rheometer (BBR) for assessing temperature sensitivity of bitumen, and the low-medium-high-temperature performances were analyzed for TiO_2/$CaCO_3$ nanoparticle-bitumen as well. Results show that bituminous mechanical properties were enhanced by TiO_2/$CaCO_3$, and based on the overall desirability analysis of various conventional tests, the reasonable dosage of nano-TiO_2/$CaCO_3$ was recommended as 5% by weight of base bitumen. Adding nano-TiO_2/$CaCO_3$ was beneficial to improve the viscosity and reduce the temperature sensitivity of bitumen. The capacities of bituminous rutting resistance as well as medium-temperature fatigue resistance were enhanced by the addition of nano-TiO_2/$CaCO_3$. However, BBR test shows that bituminous anticracking is reduced slightly. On this basis, the Burgers model is selected for clarifying the decrease in anticracking performance; that is, nano-TiO_2/$CaCO_3$ increased the stiffness modulus while increasing the viscosity of bitumen.

1. Introduction

Bituminous pavement with its superior performances has become one of the most important pavement types in China [1–4]. With the development of society, bituminous pavement-related technology and measurements have also been continuously developed, and its service performances and level have been significantly improved [5–10]. However, it is worth noting that there are yet many problems in the field of flexible pavement which need to be solved urgently. Bituminous material has a significant feature that its properties are strongly influenced by its service temperature [11–13]. The resulting damage will reduce the service performance of bituminous flexible materials, such as rutting, cracks, and other damage phenomena [2, 14–18].

In general, there are many factors affecting the performance degradation of bituminous flexible materials, including material internal factors and service condition factors [19]. A lot of related research works have been done, including modifying bituminous materials [20, 21] and optimizing bituminous flexible pavement structure [22]. However, with the rapid development of nanotechnology, more and more researchers are committed to introducing nanomaterials to modify bitumen [23]. Nanomaterials refer to materials in the range of 1~100 nanometers in at least one dimension. It has previously been observed that the physical, chemical, and other properties of nanomaterials have great differences from the original raw materials [24]. It is worth noting that nanomaterials usually have the advantages of significant temperature susceptibility, better extendability, larger specific surface area (SSA), and so on. Therefore, on the above basis, researchers introduced nanomaterials into road and construction fields. Jahromi et al. employed two kinds of nanoclay to improve the performances of bituminous materials. According to X-ray diffraction along with dynamic shear rheometer (DSR) tests, nanoclay modified bitumen increased stiffness and decreased phase angle [25]. Abdelrahma et al. assessed the physical performances of bitumen through adding the modified nanoclay using dynamic mechanical analysis and showed that the incorporation of modified nanoclay materials into bituminous materials enhanced their physical properties. Also, they investigated the modification mechanism of nanoclay, which was considered to be the interactivity of the modified nanosilica tetrahedron in bitumen using the FTIR test [26]. You et al. used nanoclay to modify bitumen and compared two kinds of nanoclay. The results indicated that nanoclay could effectively boost the comprehensive performances of bituminous materials. Furthermore, the blending procedure was considered as the key to achieving a well-distributed nanoclay modified bitumen [27]. Khattak et al. employed different dosages of carbon nanofibers to modify three types of bituminous cement based on two bituminous mixing procedures, i.e., dry and wet procedures. Due to the larger SSA and better interface combination effect as well as higher modulus values of carbon nanofiber, the test results showed that carbon nanofiber-modified bitumen exhibited good viscoelastic response and fatigue performances [28]. Chen et al. utilized nano-TiO_2 to modify bitumen through permeability technology and evaluated the penetration effect using a scanning electron microscope. Because of the large surface area and advanced oxidation technology of nano-TiO_2, nano-TiO_2-modified bitumen produced good performances of bitumen and also had a good environment purification function [29]. Because of SSA and good dispersion as well as stability of nanosilica, it was applied to medicine, engineering, and so on. It was found that the performances of bituminous materials were greatly enhanced through incorporating nanosilica [30]. Yusoff et al. thought that sensitivity to moisture damage of polymer-modified bituminous materials was decreased while their antirutting and fatigue performances were increased through incorporating nanosilica [31]. Using the mentioned nanomaterials could significantly boost the ability of bituminous flexible pavement to reply to service conditions, for instance, its antirutting and cracking [32, 33].

On the other hand, considering the typical viscoelastic-plastic characteristics of bituminous flexible pavement under its service conditions, there are still inescapable deformations [34–37]. Despite various technical measures, there are still many problems related to deformation resistance of bituminous flexible pavement including ruts, cracks, and other deformation damage phenomena, which can be attributed to the insufficient deformation resistance [38, 39]. Consequently, it is quite essential to discuss and evaluate the deformation performance of bituminous materials from the perspective of the viscoelastic constitutive model. Liu et al. proposed two methods to construct the master curves for bituminous concretes based on Kramers-Kronig relations [40]. Lagos-Varas et al. developed a new method of viscoelastic mechanical behaviors based on derivatives of fractional order, which can well describe the practical construction and be suitable for modified bitumen [41]. Wang et al. prepared the polymer and basalt fiber-modified bituminous mixtures by Superpave gyratory compaction and assessed viscoelastic properties under F-T [42]. Ma et al. performed laboratory tests and virtual creep tests based on discrete element technology for viscoelastic behavior of bituminous materials considering multiple ingredients [43]. Darabi et al. investigated viscoelastic behaviors of bituminous mixture. Then they applied laboratory experiments to verify mechanical response [44].

The objective of this work is to carry out a study on rheological performances of bitumen containing nano-TiO_2/$CaCO_3$. Firstly, a series of experiments have been performed for bitumen with different dosages of nano-TiO_2/$CaCO_3$ to confirm the nano-TiO_2/$CaCO_3$ dosage. After that, modified bitumen with optimum dosage was prepared for rotational viscosity test and DSR as well as beam bending rheometer (BBR) for assessing temperature sensitivity. Meanwhile, the low-medium-high-temperature performances of nano-TiO_2/$CaCO_3$-modified bitumen were discussed as well. On this basis, bituminous viscoelastic behavior is analyzed using the Burgers model.

2. Experimental Materials and Methods

2.1. Materials and Tested Specimens

2.1.1. Base Bitumen. The 90# base bitumen AH-90 is acquired from Panjin, China, and the main technical indicators are in Table 1.

2.1.2. Nano-TiO_2/$CaCO_3$. The nano-TiO_2/$CaCO_3$ was developed and provided by the College of Chemistry, Jilin University. Table 2 is the detailed technical characteristics. Figure 1 shows the SEM image of nano-TiO_2/$CaCO_3$.

2.1.3. TiO_2/$CaCO_3$ Nanoparticle-Bitumen. Nano-TiO_2/$CaCO_3$ was added to base bitumen to prepare nano-TiO_2/$CaCO_3$-modified bitumen with a percentage dosage of 3%, 4%, 5%, 6%, 7%, 8%, and 9% of the total base bitumen by weight [45, 46]. As shown in Figure 2, the sample preparation procedure is as follows [45, 47]: base original bituminous material was preheated to 160°C and next it was blended with modified nano-TiO_2/$CaCO_3$ with manually stirring for 5 min. The corresponding temperature increased to 170°C in a short time. Finally, the high-speed shearing was carried out with a revolution of 6000 r/min at 170°C for 40 min. Before use, heat the bitumen sample again to 170°C, control the shearing speed at 450~600 r/min, and stir continuously for 20 min.

Table 1: Indicators of AH-90.

Indicators		Methods	Tested
Penetration		T0604	95.9
Ductility	5°C	T0605	12.8
	10°C		>100
Softening point		T0606	43.0
Density		T0603	1.018
Dynamic viscosity	60°C	T0620	98.8
	135°C		0.294
RTFOT			
Mass loss	%	T0610	−0.189
Residual penetration ratio	% (@ 25°C)	T0604	85.2

Table 2: Indicators of $TiO_2/CaCO_3$ nanoparticles.

Indicators		Tested
Appearance	—	White power
Tapped density	g/cm^3	0.3
Diameter	nm	50~60
SSA	m^2/g	10
Proportion	—	20% TiO_2 + 80% $CaCO_3$

2.2. Laboratory Tests of Bitumen

2.2.1. Conventional Tests of Bitumen. The penetration test is performed to assess the consistency of bitumen, which is carried out at 25°C following JTG E20-2011 T0604. The softening point (SP) test is adopted for bituminous materials. Then using measured values, penetration index (PI) can be calculated, which generally describes and evaluates the temperature sensitivity of bitumen quantitatively. And the PI equation expression is [48]

$$\mathrm{PI} = \frac{1952 - 500\log_{10} P25 - 20\mathrm{SP}}{50\log_{10} P25 - \mathrm{SP} - 120}. \quad (1)$$

Ductility property is measured by the ductility test. Bituminous samples with standard size are stretched until broken with a stretching rate at 10°C. Ductility value is defined as the stretched distance at breaking.

In view of the above different trends of conventional physical performances of modified bitumen with various nano-$TiO_2/CaCO_3$ dosages, the overall analysis is required, and the overall desirability (OD) is selected for normalization and analysis. The conventional physical properties of modified bitumen are normalized based on different desirability, which are defined as follows [48]:

$$\gamma(k) = \left[x_1^*(k)x_2^*(k)\cdots x_m^*(k)\right]^{1/m}, \quad (2)$$

in which $x_i^{(0)}(k)$ and $x_i^*(k)$ are the k-th original and normalized values in the i-th physical property, respectively. m is the number of conventional physical properties.

2.2.2. Rotational Viscosity Test. Bitumen may exhibit non-Newtonian behavior within service temperature range and its viscosity coefficient is not constant. The Brookfield rotational viscometer was adopted, which is maintained in a chamber. As described in JTG E20-2011 T0625, the torque and rotation rate are adopted to calculate the apparent viscosity of bitumen. The test temperature is arranged from low to high.

To quantitatively express the sensitivity of bitumen to temperature, viscosity-temperature susceptibility (VTS) was adopted for assessing temperature sensitivity in this study, and its calculation equation is shown as follows:

$$\mathrm{VTS} = \frac{\lg\lg\left(\eta_2 \times 10^3\right) - \lg\lg\left(\eta_1 \times 10^3\right)}{\lg\left(T_2 + 273.13\right) - \lg\left(T_1 + 273.13\right)}, \quad (3)$$

where η_1 and η_2 are the corresponding viscosity at temperatures T_1 and T_2 (herein, $T_1 = 60°C$ and $T_2 = 135°C$).

2.2.3. Dynamic Shear Rheometer Test. DSR developed by SHRP was employed for the sake of analyzing the dynamic characteristics and evaluating the viscoelastic behavior of bituminous materials [48–50]. Compared to static experiments (penetration, softening point, etc.), the DSR test has more intuitive and real advantages to assess the properties of bituminous materials. Following the specification ASTM D7175, the rheological parameters of bituminous materials are determined by Malvern Bohlin Gemini 150.

In the DSR test, the dynamic viscoelastic behavior of bitumen can be divided into two parts, including G^* and δ [4, 51, 52]. G^* is calculated by applying dynamic shear stress ($\tau_{\max}$) to bituminous sample, $\gamma_{\max}$, defined by

$$G^* = \frac{\tau_{\max}}{\gamma_{\max}}. \quad (4)$$

The phase angle (δ) reflects the ratio of viscoelasticity in bitumen. Under the condition of high-temperature or low-frequency loading, bitumen is more prone to viscous flow, so the phase angle is larger, while under the condition of low-temperature or high-frequency loading, bitumen exhibits more elastic properties and the phase angle is smaller.

2.2.4. Beam Bending Rheometer Test. BBR test is a method for measuring the hardness of bituminous beam with a dimension of 6.25 × 12.5 × 127 mm under creep loading based on the theory of engineering beam [48]. Two parameters can be obtained from the deflection curves versus time, that is, $S(t)$ and m-value. Their equations are expressed in equations (5)–(7):

$$S(t) = \frac{Pl^3}{4bh^3u(t)}, \quad (5)$$

$$\log S(t) = A + B\lg t + C(\lg t)^2, \quad (6)$$

$$m(t) = |B + 2C\lg t|. \quad (7)$$

The flowchart of experimental design for this study is shown in Figure 3. Three replicates for each specimen were tested and measured.

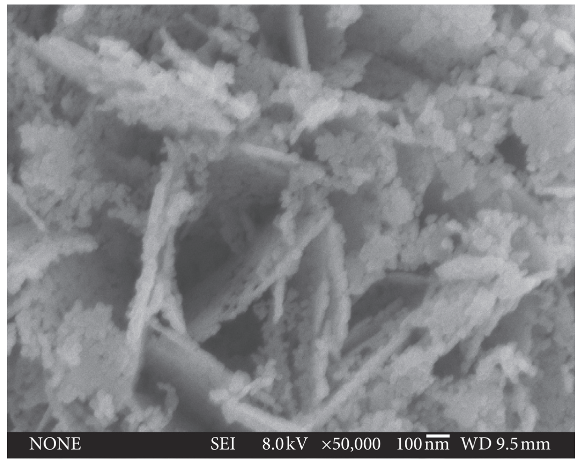

FIGURE 1: SEM image of nano-$TiO_2/CaCO_3$.

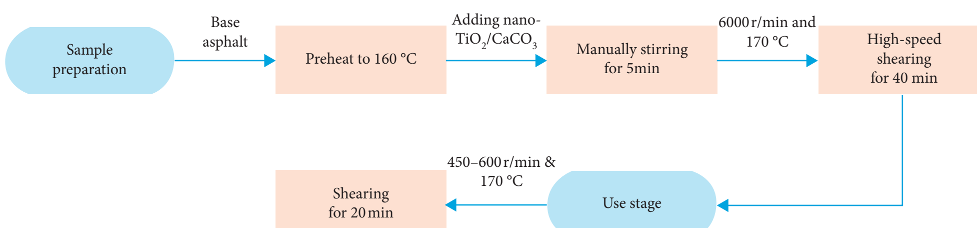

FIGURE 2: Bituminous sample preparation procedure in this study.

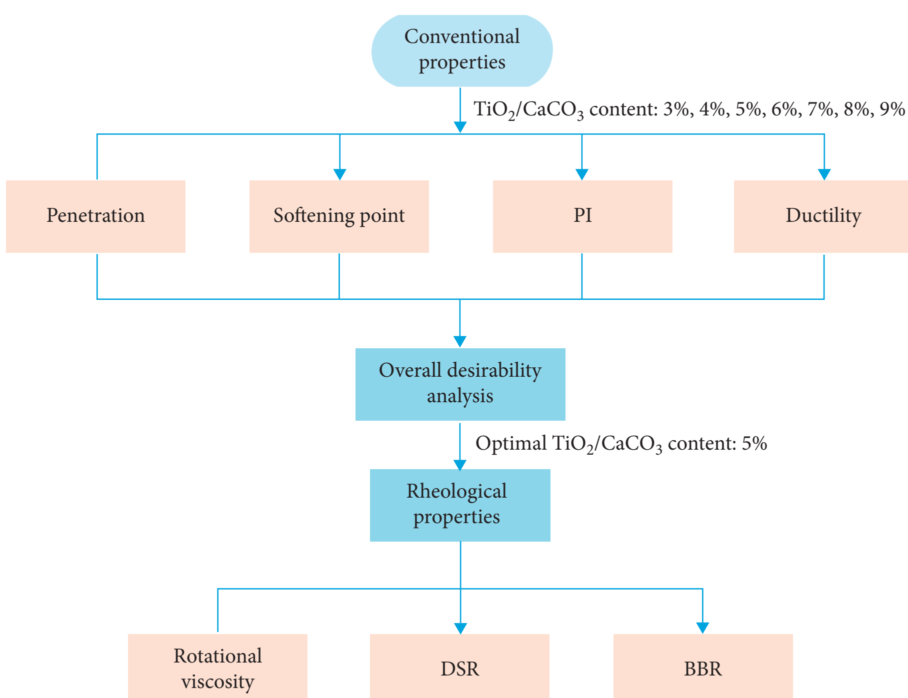

FIGURE 3: Flowchart of this study.

3. Results and Discussion

3.1. Optimum Content of Nano-$TiO_2/CaCO_3$

3.1.1. Conventional Tests of Nano-$TiO_2/CaCO_3$-Modified Bitumen. The experimental results of conventional physical performances of modified bitumen with various percentages of nano-$TiO_2/CaCO_3$ are plotted in Figure 4. It is observed that the penetration at 25°C decreases and the SP value becomes larger with the increasing of nano-$TiO_2/CaCO_3$, but their variation slope becomes smaller gradually when the percentage of nano-$TiO_2/CaCO_3$ is more than 5%. The ductility at 10°C decreases fast firstly and then decreases slowly but finally decreases significantly. The above changing trend indicates that nano-$TiO_2/CaCO_3$ would reduce the sensitivity of bitumen to temperature, which was consistent with the analysis results by Cheng et al. [53].

Penetration decreases significantly first and then tends to stabilize with nano-$TiO_2/CaCO_3$ increasing in Figure 4(a), which shows that adding nano-$TiO_2/CaCO_3$ reduced the sensitivity of bitumen to temperature. From Figure 4(b), SP increases significantly and then changes slightly when nano-$TiO_2/CaCO_3$ content increases. As shown in Figure 4(c), the PI shows a changing trend from increasing to decreasing. In addition, in Figure 4(d), the ductility of modified bitumen at 10°C also shows a changing trend of decreasing. The ductility at 10°C is the largest value at the nano-$TiO_2/CaCO_3$ content of 3%. Next, the ductility at 10°C decreases again and the variation slope increased. The ductility results indicate that nano-$TiO_2/CaCO_3$ would enhance the low-temperature extendability of modified bitumen to some extent, but the low-temperature property of modified bitumen may be damaged when the dosage of nano-$TiO_2/CaCO_3$ is too high. The modifier nano-$TiO_2/CaCO_3$ can absorb the light components in asphalt, but when the modifier content is too high, its absorption effect has already reached the best, but the effect is not significant, which was also consistent with the analysis results by Cheng et al. [53].

Table 3 presents the OD analysis. There is different desirability for different physical properties. For the OD analysis results of nano-$TiO_2/CaCO_3$-modified bitumen, the OD value ($\gamma(k)$) increases first, but the OD value becomes smaller when nano-$TiO_2/CaCO_3$ content is larger than 5%. Thus, a reasonable percentage of $TiO_2/CaCO_3$ is 5% by mass of base bitumen [48].

3.1.2. Technical Indicators of $TiO_2/CaCO_3$ Nanoparticle-Bitumen. Table 4 presents the main technical properties of nano-$TiO_2/CaCO_3$-bitumen. Adding nano-$TiO_2/CaCO_3$ decreases the penetration of modified bitumen. The 90# base bitumen with nano-$TiO_2/CaCO_3$ is equivalent to the 70# bitumen, which indicates that the consistency of the bitumen has been significantly improved. Meanwhile, the softening point of nano-$TiO_2/CaCO_3$-modified bitumen has increased by about 3°C, and the dynamic viscosity at 60°C has increased by about 6%. The high-temperature resistance of bitumen is significantly enhanced by nano-$TiO_2/CaCO_3$. The ductility reduced, indicating that modified bitumen still has a good low-temperature property.

3.2. Rotational Viscosity Test. The viscosity of bitumen was tested, which is presented in Figure 5. The slope represents bituminous sensitivity. As seen from Figure 5, the temperature sensitivity of 90# base bitumen is higher, while the nano-$TiO_2/CaCO_3$-modified bitumen reduced the temperature sensitivity.

According to equation (3), the VTS results are as follows: the VTS of base bitumen is −3.471 and the VTS of nano-$TiO_2/CaCO_3$-modified bitumen is −3.207. By comparison, the absolute VTS value of $TiO_2/CaCO_3$ nanoparticle-bitumen is smaller by comparison, which is approximately reduced by 7.6%. This indicates that nano-$TiO_2/CaCO_3$ would reduce the temperature sensitivity of bitumen. This may be because the light components in asphalt are absorbed by nanoparticles, which makes the resin and asphaltene in asphalt increase and the adhesive force increase [54]. The viscosity at 135°C (0.415 Pa•s) of nano-$TiO_2/CaCO_3$-modified bitumen does not exceed 3 Pa•s. The preparation condition for nano-$TiO_2/CaCO_3$-modified bitumen is about 5°C higher than that of base bitumen, but much lower than other types of commonly used polymer-modified bitumen, which could enhance the construction cheapness of bituminous pavement to some extent.

3.3. Dynamic Shear Rheometer Test

3.3.1. Complex Shear Modulus (G^*) and Phase Angle (δ). Bitumen has significant temperature sensitivity and has different mechanical properties at different temperatures. To explore the rheological characteristics of bituminous binder in medium- and high-temperature ranges, the DSR test was conducted at 10 rad/s, 10~80°C, and the strain was controlled as 12%. The measured G^* and δ versus temperature were plotted in Figure 6.

Values G^* decrease with test temperature increasing. Because bituminous fluidity rises with temperature, and it is prone to show more significant deformation at the same stress level. Clearly, a higher complex shear modulus is generally required to ensure that bituminous pavement still has a good resistance to high-temperature deformation. Furthermore, the complex shear modulus of nano-$TiO_2/CaCO_3$-modified bitumen is 4.8% lower at 10°C, while by comparison, the complex shear modulus of nano-$TiO_2/CaCO_3$-modified bitumen is 12.8% higher at 80°C. This indicates that the nano-$TiO_2/CaCO_3$-modified bitumen has higher temperature stability than base original bitumen due to the higher complex shear modulus at high temperatures.

The characteristics (δ) is the relative indicatrix between recoverable and unrecoverable deformation, in which $\delta = 0°$ for elastic solids and $\delta = 90°$ for viscous fluids. Values δ of base as well as nano-$TiO_2/CaCO_3$-modified bitumen increase as test temperature increases, which fully reflects the characteristics of a viscous fluid for bitumen as a typical viscoelastic material. The phase angle of base bitumen changes 28.3°, and the δ values change 26.2° for the modified bitumen. This indicates that nano-$TiO_2/CaCO_3$-bitumen possesses little sensitivity compared with base one. Moreover, since flow deformation of nano-$TiO_2/CaCO_3$-modified

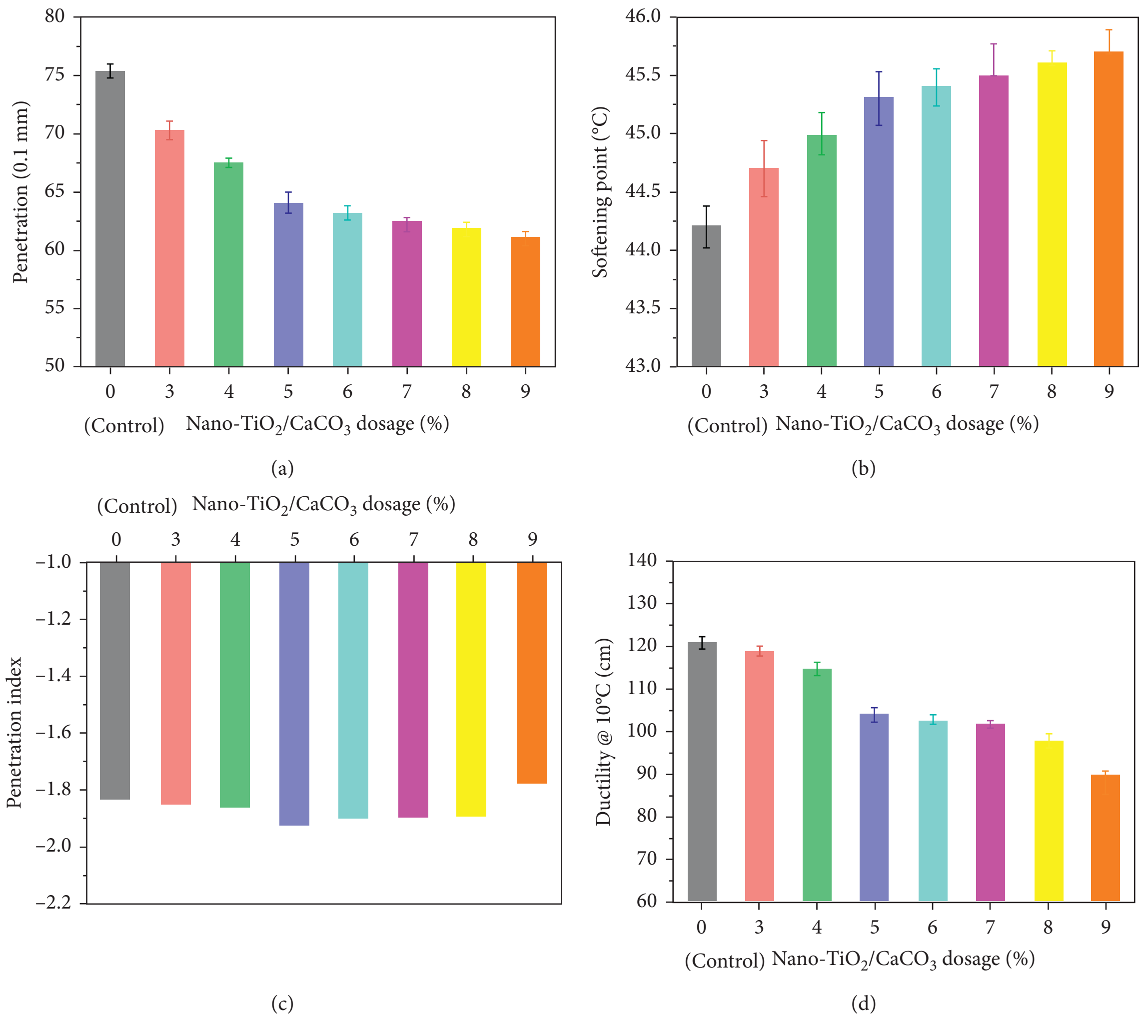

Figure 4: Conventional physical properties of bituminous samples with different nano-$TiO_2/CaCO_3$ dosage. (a) Penetration, (b) SP, (c) PI, and (d) ductility.

Table 3: The OD analysis of nano-$TiO_2/CaCO_3$-modified bitumen.

Nano-$TiO_2/CaCO_3$ dosage	Normalization				OD $\gamma(k)$
	Penetration	Softening point	PI	Ductility	
0	0	0	0	1	0
3	0.356643	0.333333	0.231592	0.935691	0.400629
4	0.552448	0.533333	0.327327	0.800643	0.527142
5	0.839161	0.733333	1	0.453376	0.726777
6	0.853147	0.8	0.755845	0.421222	0.682754
7	0.902098	0.866667	0.721288	0.379421	0.680118
8	0.944056	0.933333	0.648298	0.266881	0.624858
9	1	1	0.662905	0	0

Table 4: Technical properties of nano-$TiO_2/CaCO_3$-modified bitumen.

Indicators		Methods	Tested
Penetration		T0604	63.5
Ductility	5°C	10.3	12.8
	10°C	84.7	>100
Softening point		T0606	45.3
Density		T0603	1.028
Dynamic viscosity	60°C	104.9	98.8
	135°C		0.294
RTFOT			
Mass loss	%	T0610	−0.199
Residual penetration ratio	% (@ 25°C)	T0604	95.0

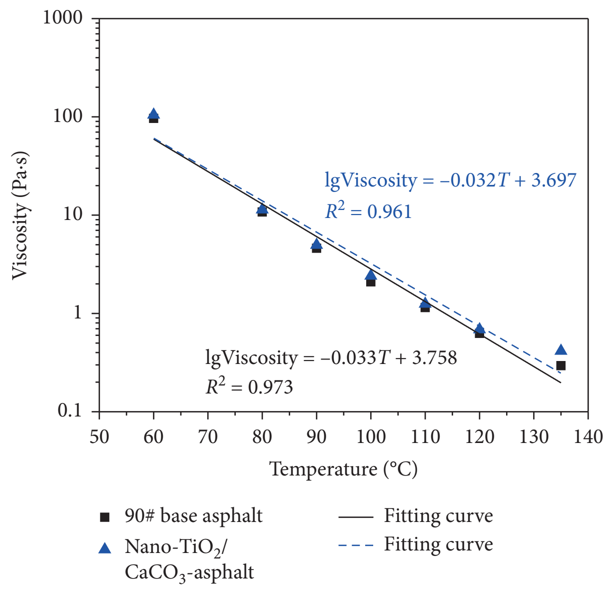

Figure 5: The viscosity-temperature curve of base bitumen and nano-$TiO_2/CaCO_3$-modified bitumen.

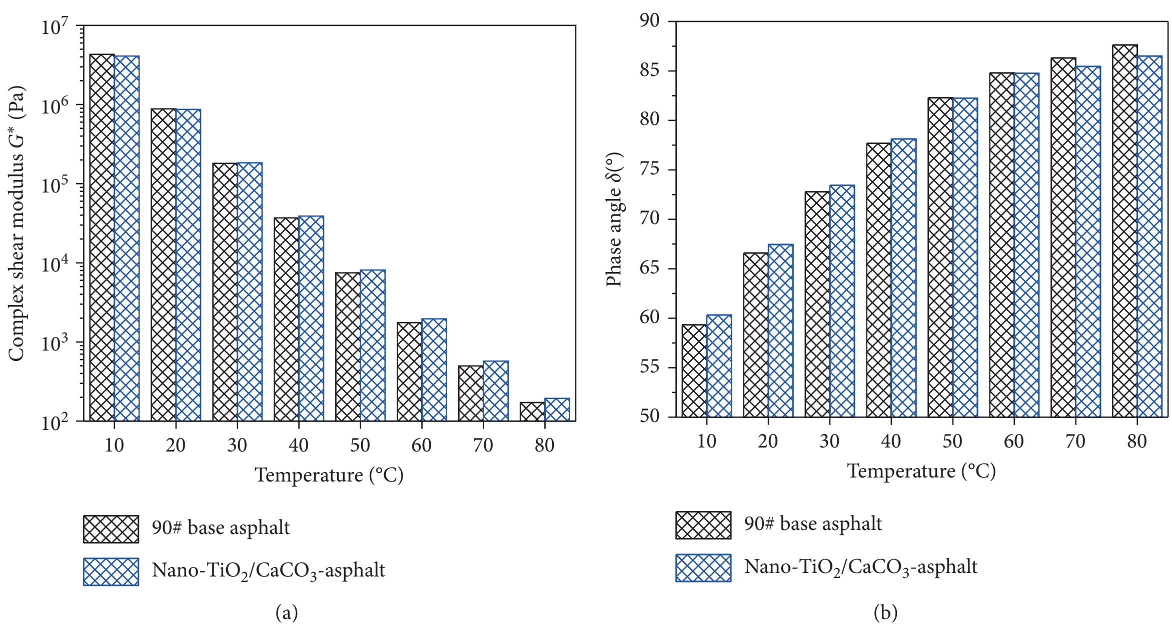

Figure 6: DSR results versus temperatures. (a) G^* and (b) δ.

bitumen at high temperature is smaller, nano-$TiO_2/CaCO_3$ is beneficial for bituminous pavement to resist high-temperature deformation.

Taking 60°C as the reference temperature, the complex shear modulus of base bitumen and nano-$TiO_2/CaCO_3$-modified bitumen is plotted in Figure 7. As shown, the complex modulus of base bitumen and nano-$TiO_2/CaCO_3$-modified bitumen is frequency-dependent, and their complex modulus increases with reduced frequency. At the same reduced frequency, the complex modulus of nano-$TiO_2/CaCO_3$-modified bitumen is higher. Moreover, the higher the frequency, the more significant their difference. Since the frequency relates to temperature, it also indicates that nano-$TiO_2/CaCO_3$ could boost the stabilization capability at higher temperature [52].

3.3.2. Rutting Factor ($G^*/sin\delta$) and Fatigue Factor ($G^*sin\delta$). It is only one-sided to assess the properties of bitumen from the perspective of G^* or δ. If G^* is the same, their phase angle values may not be the same, and vice versa. Therefore, it needs to use different indicators to evaluate the performance of bitumen for various performances at different test temperatures.

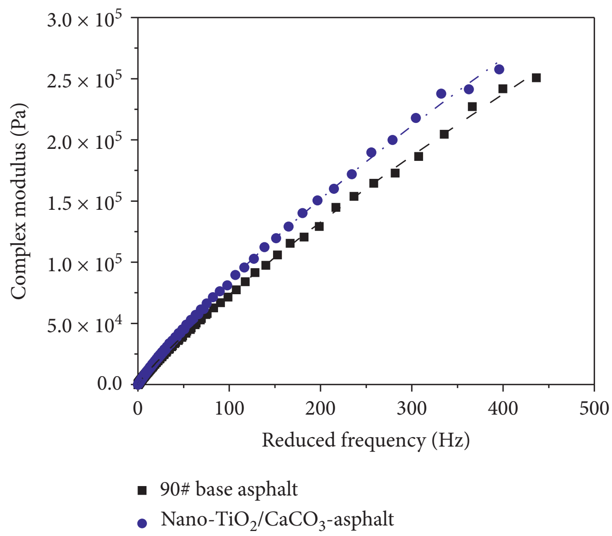

Figure 7: Master curve of complex modulus for base bitumen and nano-$TiO_2/CaCO_3$-modified bitumen.

Most studies have shown that the loss modulus ($G'' = G^* \sin\delta$) has an important relationship with the fatigue characteristics of bitumen and bituminous mixtures. The larger the value of $G^* \sin\delta$, the faster the energy loss under repeated loads and the lower the resistance to fatigue damage of bitumen and bituminous mixtures. Thus, $G^* \sin\delta$ is called the fatigue factor. On the other hand, $G^*/\sin\delta$ represents the rutting factor. Therefore, compared to static tests (such as penetration and softening point), dynamic tests have more intuitive and real advantages to evaluate the performances of bituminous binders.

Bituminous pavement is generally taken as 40°C~80°C, and the rutting factor results of base bitumen and nano-$TiO_2/CaCO_3$-modified bitumen are plotted in Figure 8(a). As seen, the rutting factor of nano-$TiO_2/CaCO_3$-modified bitumen is larger by comparison at the same test temperature, which means that nano-$TiO_2/CaCO_3$-modified bitumen has a better high-temperature antirutting ability than base bitumen. Moreover, compared with base bitumen, the growth rate of rutting factor for nano-$TiO_2/CaCO_3$-modified bitumen changes from 5% to 13% when the test temperature increases from 40°C to 80°C [55].

Bituminous pavement usually services at a medium-temperature level. Therefore, bituminous materials need to have good antifatigue properties to maintain good working performance for a long period. As mentioned in the literature review, the smaller the fatigue factor, the better the fatigue resistance of bitumen. The fatigue factor results of base bitumen and nano-$TiO_2/CaCO_3$ modified bitumen are plotted in Figure 8(b). The fatigue factors of nano-$TiO_2/CaCO_3$-modified bitumen are lower to different degrees at 10°C~30°C. This shows that nano-$TiO_2/CaCO_3$-modified bitumen also has good fatigue resistance properties at medium temperature. The energy loss of nano-$TiO_2/CaCO_3$-modified bitumen is slower under repeated loads, and it can continue to work for a longer time.

3.4. Beam Bending Rheometer Test

3.4.1. BBR Test Analysis

(1) Creep Characteristics. The creep deformations versus loading time at −18°C for base bitumen and nano-$TiO_2/CaCO_3$-modified bitumen were measured. The deflection-time curve reflects a typical viscoelastic behavior of bitumen in Figure 9. Nano-$TiO_2/CaCO_3$-modified bitumen and base bitumen have similar creep curves. Stage I: at the initial loading, these two kinds of bitumen have obvious elastic deformation, which characterizes the low-temperature elastic performances of bitumen. Stage II: within 50 s of loading, the deformation of bitumen gradually increases, and the growth rate of deformation gradually decreases. This is due to the combined effect of the viscous and elastic properties of bitumen. Stage III: from 50 s to the end of loading, the deformation of bitumen continues to increase, and the growth rate of deformation tends to be constant, representing the viscous nature of bitumen. Stage IV: after unloading, bitumen shows an instantaneous elastic recovery and a delayed elastic recovery.

Although the creep characteristics of base bitumen and nano-$TiO_2/CaCO_3$-modified bitumen are not essentially different, their proportion of viscoelastic components have been changed. Under the same constant load, the deformation of nano-$TiO_2/CaCO_3$-modified bitumen is smaller by comparison.

(2) Stiffness Modulus and m-Value. In SHRP specifications, modulus as well as its m-value is recommended as a basis for PG performance classification. The larger the corresponding creep stiffness modulus, that is, the smaller the creep deformation, the greater the stress required to produce unit strain, indicating that the bituminous material is harder. Figure 10 plots the creep stiffness modulus and m-value varying with time for base bitumen and nano-$TiO_2/CaCO_3$-modified bitumen. Creep stiffness modulus for base bitumen and nano-$TiO_2/CaCO_3$-modified bitumen decreases with time. However, the creep stiffness modulus of nano-$TiO_2/CaCO_3$-modified bitumen is larger by comparison and not more than 300 MPa, which meets the specification requirements. In Figure 10(b), the m-value of base bitumen and nano-$TiO_2/CaCO_3$-modified bitumen becomes larger as time goes on. The m-value at 60 s of nano-$TiO_2/CaCO_3$-modified bitumen is smaller, and the m-value is larger than or equal to 0.3, meeting the specification requirements. This is mainly because the light components in asphalt are absorbed by nanoparticles, which increases the relative proportion of heavy components and makes asphalt more hard and brittle [53]. Compared with base bitumen, nano-$TiO_2/CaCO_3$-modified bitumen has a larger modulus with a smaller m-value, representing that crack resistance for modified bitumen has been reduced slightly, but it can also meet the specification requirements.

3.4.2. Rheological Model of Bitumen. The modulus versus loading time can be fitted by taking the logarithm of stiffness modulus and time according to equation (6), and the SHRP

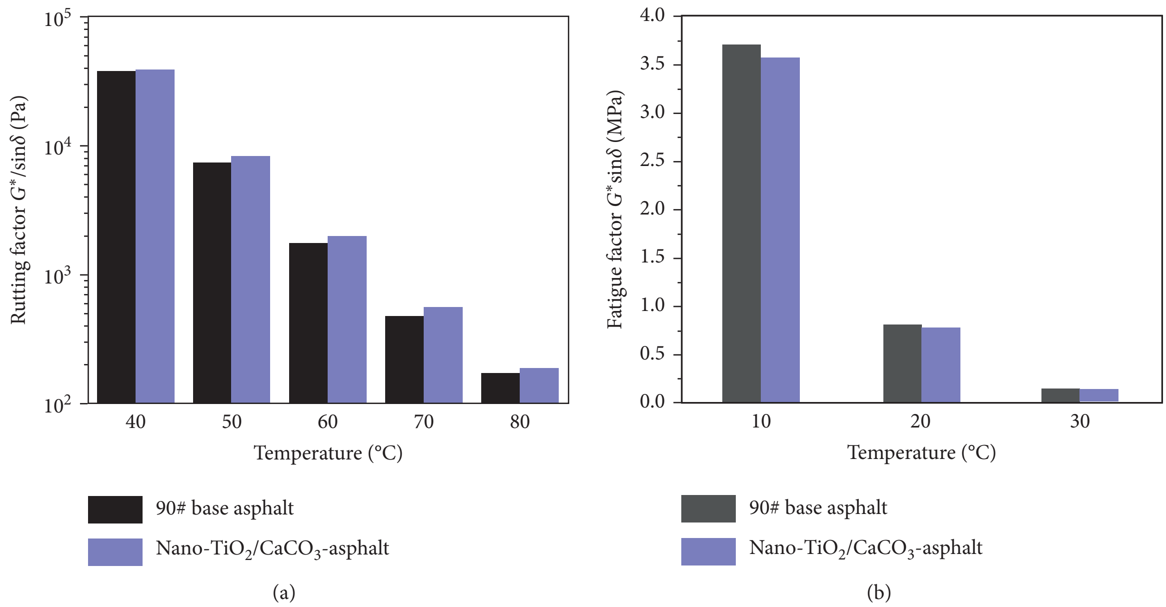

Figure 8: Deformability of base bitumen and nano-$TiO_2/CaCO_3$-modified bitumen. (a) $G^*/\sin\delta$ and (b) $G^*\sin\delta$.

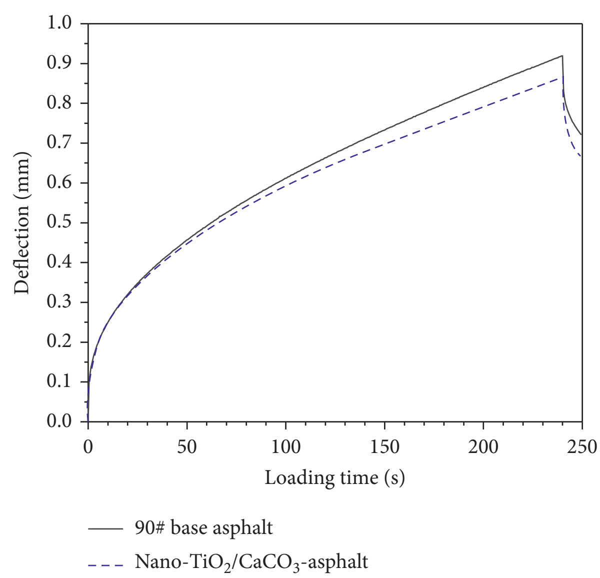

Figure 9: Creep curve of base bitumen and nano-$TiO_2/CaCO_3$-modified bitumen.

models of base bitumen and nano-$TiO_2/CaCO_3$-modified bitumen are plotted in Figures 11(a) and 11(b), respectively. Although the accuracy of the fitting SHRP model is high, these fitted parameters do not have clear physical meaning, which could not reflect viscoelastic properties of bituminous materials.

Prior studies have noted the effectiveness of the Burgers model for bitumen [42]. The Burgers model of stiffness modulus of small bituminous binder beam was defined:

$$S(t) = \left(\frac{t}{\eta_1} + \frac{1}{E_1} + \frac{1}{E_2}\left(1 - e^{-(E_2/\eta_2)t}\right)\right)^{-1}. \quad (8)$$

The Burgers model has been obtained by fitting the following equation (8), as shown in Figure 11. E_1 of nano-$TiO_2/CaCO_3$-modified bitumen is larger by comparison, which shows that the instant elastic deformation of modified bitumen is smaller compared with base bitumen. η_1 is the viscosity coefficient for permanent deformation, and a larger value of η_1 represents the smaller permanent deformation. η_1 of $TiO_2/CaCO_3$ nanoparticle-bitumen was slightly larger by comparison, which means that incorporation of nano-TiO_2/$CaCO_3$ increases the viscosity of bitumen and reduces its creep rate. In addition, E_2 is important for preventing the development of viscous element η_2, and these two

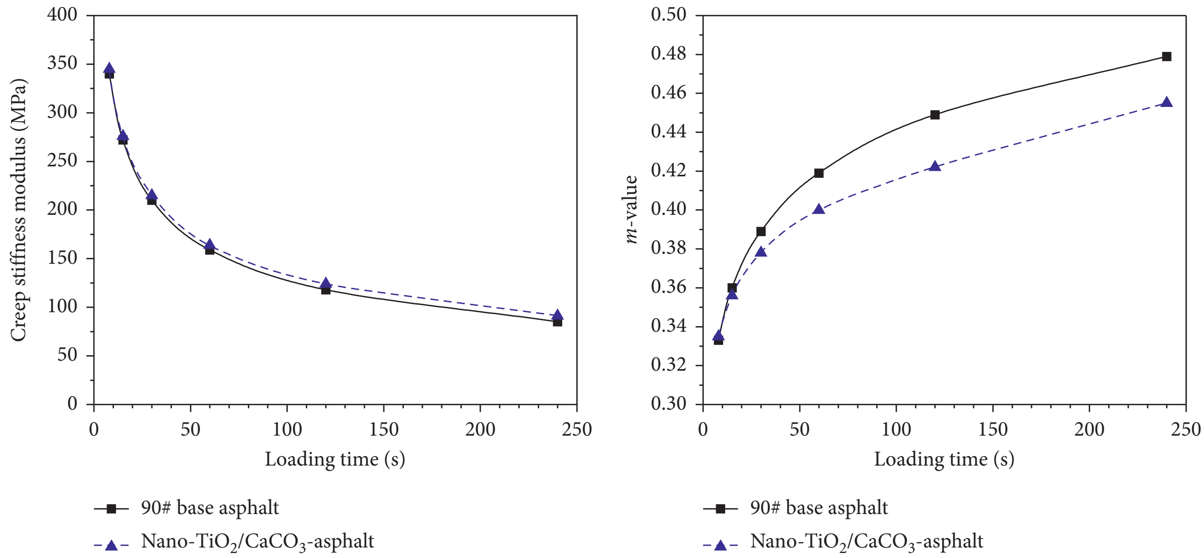

(a) (b)

Figure 10: BBR comparison analysis. (a) Modulus and (b) m-value.

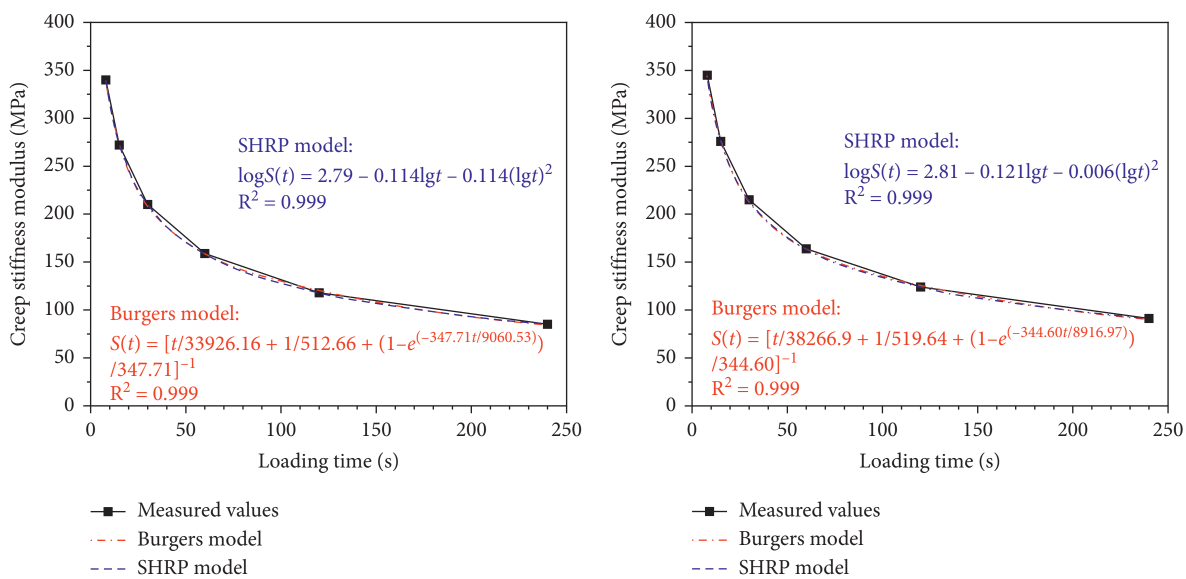

(a) (b)

Figure 11: Rheological models of bitumen. (a) Base bitumen and (b) nano-$TiO_2/CaCO_3$-modified bitumen.

parameters are mainly reflected in the initial stages of loading and unloading. In general, by comparing Figures 11(a) and 11(b), there is little difference for the stiffness modulus and m-value between base bitumen and nano-$TiO_2/CaCO_3$-modified bitumen. Nano-$TiO_2/CaCO_3$-modified bitumen has very slight changes in increasing stiffness modulus and reducing deformation. Therefore, the incorporation of nano-$TiO_2/CaCO_3$ has little effect on improving the anticracking property of bitumen at low temperature.

In addition, both the SHRP double logarithmic polynomial fitting model and the Burgers model have high accuracy and are very close to the measured stiffness modulus. However, compared with SHRP, fitting Burgers can reflect bituminous viscoelastic changes before and after nano-$TiO_2/CaCO_3$ modification, indicating a clearer physical meaning. Therefore, it is recommended to use the Burgers model to fit and analyze the BBR test.

4. Conclusions

Influences of $TiO_2/CaCO_3$ nanoparticles on bituminous conventional performances were analyzed. Moreover, the rotational viscosity test has been employed for discussing the influences of nano-$TiO_2/CaCO_3$ on temperature sensitivity of bitumen. Meanwhile, the DSR and BBR tests were also employed to analyze the low-medium-high-temperature performances of $TiO_2/CaCO_3$ nanoparticle-bitumen. The conclusions are drawn as follows:

(1) Nano-$TiO_2/CaCO_3$ would enhance bituminous mechanical performances. As nano-$TiO_2/CaCO_3$ dosage increased, penetration and ductility of nano-$TiO_2/CaCO_3$-modified bitumen decreased, while softening point increased. When the nano-$TiO_2/CaCO_3$ dosage exceeded 5%, the growth rates of conventional test results have been slowed down. Based on the OD analysis, the reasonable dosage of nano-$TiO_2/CaCO_3$ was recommended as 5% by weight of base bitumen.

(2) According to the analysis of rotational viscosity test, the addition of nano-$TiO_2/CaCO_3$ was beneficial to improve the viscosity and reduce bituminous sensitivity. Meanwhile, viscosity variation showed a significant increasing trend.

(3) Nano-$TiO_2/CaCO_3$ can affect the G^* as well as δ but will not change its variation law with temperature. The addition of nano-$TiO_2/CaCO_3$ was beneficial to enhance the capacity of antirutting by increasing its rutting factor. The fatigue factor showed that $TiO_2/CaCO_3$ enhanced bituminous medium-temperature fatigue resistance.

(4) The proportion of viscoelastic components of bitumen was changed by $TiO_2/CaCO_3$, which changed the elastic component and viscosity component. In addition, nano-$TiO_2/CaCO_3$-modified bitumen had a larger creep stiffness modulus and a smaller m-value compared with base bitumen. It showed that anticracking property of bitumen reduced slightly but could also comply with the specification.

(5) The analysis results showed that nano-$TiO_2/CaCO_3$ could increase the stiffness modulus while increasing the viscosity of modified bitumen. Therefore, incorporating nano-$TiO_2/CaCO_3$ may weaken the low-temperature anticracking property of bitumen.

This study only evaluated the macroscopic properties of nano-$TiO_2/CaCO_3$-modified asphalt and did not conduct in-depth analysis from the aspect of microscopic mechanism, which is also the future direction of this research work.

Data Availability

The data used to support the findings of this study are available from the corresponding author upon request.

Conflicts of Interest

The authors declare that they have no conflicts of interest.

Acknowledgments

This research was funded by the Nanning Excellent Young Scientist Program (Grant no. RC20180108), Nanning Excellent Young Scientist Program and Guangxi Beibu Gulf Economic Zone Major Talent Program (Grant no. RC20190206), Science & Technology Base & Talent Special Project of Guangxi Province (Grant no. AD19245152), "Yongjiang Plan" of Nanning Leading Talents in Innovation and Entrepreneurship (Grant no. 2018-01-04), Scientific and Technological Project of Science and Technology Department of Jilin Province (Grant no. 20190303052SF), and the Innovation Special Project of Zhongshan Science and Technology Bureau (Grant no. 2019AG001).

References

[1] T. Chen, Y. C. Luan, T. Ma et al., "Mechanical and microstructural characteristics of different interfaces in cold recycled mixture containing cement and asphalt emulsion," *Journal of Cleaner Production*, vol. 258, 2020.

[2] X. H. Ding, T. Ma, L. H. Gu et al., "Investigation of surface micro-crack growth behavior of asphalt mortar based on the designed innovative mesoscopic test," *Materials & Design*, vol. 185, 2020.

[3] F. L. Tang, T. Ma, Y. S. Guan et al., "Parametric modeling and structure verification of asphalt pavement based on BIM-ABAQUS," *Automation in Construction*, vol. 111, 2020.

[4] M. Guo, M. Liang, Y. Jiao, W. Zhao, Y. Duan, and H. Liu, "A review of phase change materials in asphalt binder and asphalt mixture," *Construction and Building Materials*, vol. 258, Article ID 119565, 2020.

[5] M. Chen, B. Javilla, W. Hong et al., "Rheological and interaction analysis of asphalt binder, mastic and mortar," *Materials*, vol. 12, no. 1, 2019.

[6] A. Behnood and M. Modiri Gharehveran, "Morphology, rheology, and physical properties of polymer-modified asphalt binders," *European Polymer Journal*, vol. 112, pp. 766–791, 2019.

[7] Q. Guo, L. Li, Y. Cheng, Y. Jiao, and C. Xu, "Laboratory evaluation on performance of diatomite and glass fiber compound modified asphalt mixture," *Materials & Design (1980–2015)*, vol. 66, pp. 51–59, 2015.

[8] F. L. Tang, T. Ma, J. H. Zhang et al., "Integrating three-dimensional road design and pavement structure analysis based on BIM," *Automation in Construction*, vol. 113, 2020.

[9] M. Guo, H. Q. Liu, Y. B. Jiao et al., "Effect of WMA-rap technology on pavement performance of asphalt mixture: a state-of-the-art review," *Journal of Cleaner Production*, vol. 266, 2020.

[10] G. Tan, Z. Zhu, W. Wang et al., "Flexural ductility and crack-controlling capacity of polypropylene fiber reinforced ECC thin sheet with waste superfine river sand based on acoustic emission analysis," *Construction and Building Materials*, vol. 277, 2021.

[11] Q. L. Guo, Q. Liu, P. Zhang et al., "Temperature and pressure dependent behaviors of moisture diffusion in dense asphalt mixture," *Construction and Building Materials*, vol. 246, 2020.

[12] Y. Jiao, L. Fu, W. Shan, and S. Liu, "Damage fracture characterization of pervious asphalt considering temperature effect based on acoustic emission parameters," *Engineering Fracture Mechanics*, vol. 210, pp. 147–159, 2019.

[13] H. Xu, W. Guo, and Y. Tan, "Permeability of asphalt mixtures exposed to freeze-thaw cycles," *Cold Regions Science and Technology*, vol. 123, pp. 99–106, 2016.

[14] J. P. Bilodeau, J. Y. Yi, and P. M. Thiam, "Surface deflection analysis of flexible pavement with respect to frost penetration," *Journal of Cold Regions Engineering*, vol. 33, no. 4, 2019.

[15] L. Garcia-Gil, R. Miró, and F. E. Pérez-Jiménez, "New approach to characterize cracking resistance of asphalt binders," *Construction and Building Materials*, vol. 166, pp. 50–58, 2018.

[16] Q. L. Guo, H. Y. Wang, Y. Gao et al., "Investigation of the low-temperature properties and cracking resistance of fiber-reinforced asphalt concrete using the dic technique," *Engineering Fracture Mechanics*, vol. 229, 2020.

[17] Q. Guo, G. Li, Y. Gao et al., "Experimental investigation on bonding property of asphalt-aggregate interface under the actions of salt immersion and freeze-thaw cycles," *Construction and Building Materials*, vol. 206, pp. 590–599, 2019.

[18] G. J. Tan, W. S. Wang, Y. C. Cheng et al., "Establishment of complex modulus master curves based on generalized sigmoidal model for freeze-thaw resistance evaluation of basalt fiber-modified asphalt mixtures," *Polymers*, vol. 12, no. 8, 2020.

[19] F. Saeed, M. Rahman, D. Chamberlain, and P. Collins, "Asphalt surface damage due to combined action of water and dynamic loading," *Construction and Building Materials*, vol. 196, pp. 530–538, 2019.

[20] L. Brasileiro, F. Moreno-Navarro, R. Tauste-Martinez et al., "Reclaimed polymers as asphalt binder modifiers for more sustainable roads: a review," *Sustainability*, vol. 11, no. 3, 2019.

[21] W. S. Wang, Y. C. Cheng, H. P. Chen et al., "Study on the performances of waste crumb rubber modified asphalt mixture with eco-friendly diatomite and basalt fiber," *Sustainability*, vol. 11, no. 19, 2019.

[22] W. S. Wang, Y. C. Cheng, and G. J. Tan, "Design optimization of SBS-modified asphalt mixture reinforced with eco-friendly basalt fiber based on response surface methodology," *Materials*, vol. 11, no. 8, 2018.

[23] Z. B. Ren, Y. Q. Zhu, Q. Wu et al., "Enhanced storage stability of different polymer modified asphalt binders through nano-montmorillonite modification," *Nanomaterials*, vol. 10, no. 4, 2020.

[24] H. N. Yu, W. Dai, G. P. Qian et al., "The nox degradation performance of nano-TiO_2 coating for asphalt pavement," *Nanomaterials*, vol. 10, no. 5, 2020.

[25] S. G. Jahromi and A. Khodaii, "Effects of nanoclay on rheological properties of bitumen binder," *Construction and Building Materials*, vol. 23, no. 8, pp. 2894–2904, 2009.

[26] M. Abdelrahman, D. R. Katti, A. Ghavibazoo et al., "Engineering physical properties of asphalt binders through nanoclay-asphalt interactions," *Journal of Materials in Civil Engineering*, vol. 26, no. 12, 2014.

[27] Z. You, J. Mills-Beale, J. M. Foley et al., "Nanoclay-modified asphalt materials: preparation and characterization," *Construction and Building Materials*, vol. 25, no. 2, pp. 1072–1078, 2011.

[28] M. J. Khattak, A. Khattab, H. R. Rizvi, and P. Zhang, "The impact of carbon nano-fiber modification on asphalt binder rheology," *Construction and Building Materials*, vol. 30, pp. 257–264, 2012.

[29] M. Chen and Y. H. Liu, "Nox removal from vehicle emissions by functionality surface of asphalt road," *Journal of Hazardous Materials*, vol. 174, no. 1–3, pp. 375–379, 2010.

[30] H. Yao, Z. You, L. Li et al., "Rheological properties and chemical bonding of asphalt modified with nanosilica," *Journal of Materials in Civil Engineering*, vol. 25, no. 11, pp. 1619–1630, 2013.

[31] N. I. M. Yusoff, A. A. S. Breem, H. N. M. Alattug, A. Hamim, and J. Ahmad, "The effects of moisture susceptibility and ageing conditions on nano-silica/polymer-modified asphalt mixtures," *Construction and Building Materials*, vol. 72, pp. 139–147, 2014.

[32] S. Tayfur, H. Ozen, and A. Aksoy, "Investigation of rutting performance of asphalt mixtures containing polymer modifiers," *Construction and Building Materials*, vol. 21, no. 2, pp. 328–337, 2007.

[33] H. Wang, Z. You, J. Mills-Beale, and P. Hao, "Laboratory evaluation on high temperature viscosity and low temperature stiffness of asphalt binder with high percent scrap tire rubber," *Construction and Building Materials*, vol. 26, no. 1, pp. 583–590, 2012.

[34] H. Zhu and L. Sun, "A viscoelastic-viscoplastic damage constitutive model for asphalt mixtures based on thermodynamics," *International Journal of Plasticity*, vol. 40, pp. 81–100, 2013.

[35] X. Ma, H. Chen, G. Cao, M. Xing, and D. Niu, "Investigation of viscoelastoplastic behavior of asphalt mastic: effects of shear strain rate and filler volume fraction," *Construction and Building Materials*, vol. 200, pp. 559–569, 2019.

[36] M. Guo, Y. Tan, and S. Zhou, "Multiscale test research on interfacial adhesion property of cold mix asphalt," *Construction and Building Materials*, vol. 68, pp. 769–776, 2014.

[37] J. Q. Zhu, T. Ma, J. W. Fan et al., "Experimental study of high modulus asphalt mixture containing reclaimed asphalt pavement," *Journal of Cleaner Production*, vol. 263, 2020.

[38] K. Chung, S. Lee, M. Park, P. Yoo, and Y. Hong, "Preparation and characterization of microcapsule-containing self-healing asphalt," *Journal of Industrial and Engineering Chemistry*, vol. 29, pp. 330–337, 2015.

[39] X. Zhou, B. Ma, K. Wei et al., "Preparation of shape memory epoxy resin for asphalt mixtures and its influences on the main pavement performance," *Construction and Building Materials*, vol. 267, Article ID 121055, 2020.

[40] H. Liu and R. Luo, "Development of master curve models complying with linear viscoelastic theory for complex moduli of asphalt mixtures with improved accuracy," *Construction and Building Materials*, vol. 152, pp. 259–268, 2017.

[41] M. Lagos-Varas, D. Movilla-Quesada, J. P. Arenas et al., "Study of the mechanical behavior of asphalt mixtures using fractional rheology to model their viscoelasticity," *Construction and Building Materials*, vol. 200, pp. 124–134, 2019.

[42] W. S. Wang, G. J. Tan, C. Y. Liang et al., "Study on viscoelastic properties of asphalt mixtures incorporating SBS polymer and basalt fiber under freeze-thaw cycles," *Polymers*, vol. 12, no. 8, 2020.

[43] T. Ma, H. Wang, D. Zhang, and Y. Zhang, "Heterogeneity effect of mechanical property on creep behavior of asphalt mixture based on micromechanical modeling and virtual creep test," *Mechanics of Materials*, vol. 104, pp. 49–59, 2017.

[44] M. K. Darabi, C.-W. Huang, M. Bazzaz, E. A. Masad, and D. N. Little, "Characterization and validation of the nonlinear viscoelastic-viscoplastic with hardening-relaxation constitutive relationship for asphalt mixtures," *Construction and Building Materials*, vol. 216, pp. 648–660, 2019.

[45] Y. Gong, H. Bi, Z. Tian, and G. Tan, "Pavement performance investigation of nano-TiO_2/$CaCO_3$ and basalt fiber composite modified asphalt mixture under freeze–thaw cycles," *Applied Sciences*, vol. 8, no. 12, p. 2581, 2018.

[46] W. Wang, Y. Cheng, G. Tan, and C. Shi, "Pavement performance evaluation of asphalt mixtures containing oil shale

waste," *Road Materials and Pavement Design*, vol. 21, no. 1, pp. 179–200, 2020.

[47] L. Sun, X. Xin, and J. Ren, "Asphalt modification using nanomaterials and polymers composite considering high and low temperature performance," *Construction and Building Materials*, vol. 133, pp. 358–366, 2017.

[48] W. Wang, Y. Cheng, G. Tan, Z. Liu, and C. Shi, "Laboratory investigation on high- and low-temperature performances of asphalt mastics modified by waste oil shale ash," *Journal of Material Cycles and Waste Management*, vol. 20, no. 3, pp. 1710–1723, 2018.

[49] Y. C. Cheng, W. S. Wang, G. J. Tan et al., "Assessing high- and low-temperature properties of asphalt pavements incorporating waste oil shale as an alternative material in Jilin province, China," *Sustainability*, vol. 10, no. 7, 2018.

[50] Y. Zhang, T. Ma, M. Ling et al., "Predicting dynamic shear modulus of asphalt mastics using discretized-element simulation and reinforcement mechanisms," *Journal of Materials in Civil Engineering*, vol. 31, no. 8, 2019.

[51] G. J. Tan, W. S. Wang, Y. C. Cheng et al., "Master curve establishment and complex modulus evaluation of SBS-modified asphalt mixture reinforced with basalt fiber based on generalized sigmoidal model," *Polymers*, vol. 12, no. 7, 2020.

[52] C. Wu, L. Li, W. Wang et al., "Experimental characterization of viscoelastic behaviors of nano-tio2/caco3 modified asphalt and asphalt mixture," *Nanomaterials (Basel)*, vol. 11, no. 1, 2021.

[53] Y. C. Cheng, H. P. Bi, G. R. Ma et al., "Pavement performance of nano materials-basalt fiber compound modified asphalt binder," *Journal of Jilin University (Engineering and Technology Edition)*, vol. 2, pp. 460–465, 2018.

[54] I. R. Segundo, S. Landi, A. Margaritis et al., "Physicochemical and rheological properties of a transparent asphalt binder modified with nano-TiO_2," *Nanomaterials*, vol. 10, no. 11, p. 2152, 2020.

[55] G. Qian, H. Yu, X. Gong, and L. Zhao, "Impact of nano-TiO_2 on the No_2 degradation and rheological performance of asphalt pavement," *Construction and Building Materials*, vol. 218, pp. 53–63, 2019.